British Journal of Medicine & Medical Research
3(3): 654-680, 2013

SCIENCEDOMAIN *international*
www.sciencedomain.org

Stromal Stem Cells from Parathyroid Glands of Patients with Secondary Hyperparathyroidism Demonstrate Higher Telomerase Activity and Osteogenic Differentiation Ability than Normal Bone Marrow Derived Stromal Stem Cells

Erdal Karaöz[1*], Soykan Arıkan[2], Ayça Aksoy[1], Zehra Seda Ünal[1], Mine Adaş[3], Gökhan Adaş[4] and Gökhan Duruksu[1]

[1]Center for Stem Cell and Gene Therapy Research and Practice, Kocaeli University. Turkey.
[2]Istanbul Education and Research Hospital, Department of Surgery. Turkey.
[3]Okmeydani Education and Research Hospital, Department of Endocrinology. Turkey.
[4]Bakırköy Dr. Sadi Konuk Education and Research Hospital, Department of Surgery, Turkey.

Authors' contributions

This work was carried out in collaboration between all authors. Author EK was involved in the study conception and design of the study. Authors EK and GD had role in the analysis and interpretation of data, and drafting of the manuscript. Author SA had contributions in the study conception and design. Authors AA and ZSU helped in the acquisition of data, and authors MA and GA in critical revision of the manuscript. All authors read and approved the final manuscript.

Research Article

Received 31st October 2012
Accepted 16th January 2013
Published 28th February 2013

ABSTRACT

Aims: The aim of this study was to isolate and extensively characterize parathyroid gland stem cells (PT-SCs) from secondary hyperparathyroidism cases. For this purpose, proliferation capacity, phenotypic properties, differentiation characteristics and gene expression profiles were analyzed and compared with mesenchymal stem cells from bone marrow (BM-MSCs) of the human.
Methods: Stem cells isolated from PT and BM were analyzed by flow cytometry, RT-PCR, Real Time-PCR, and immunocytochemistry. Both cell lines were directionally

**Corresponding author: Email: ekaraoz@hotmail.com;*

differentiated towards adipogenic, osteogenic and neurogenic cell lineages.
Results: The isolated hPT-SCs share similar characteristics of hBM-MSCs by immunophenotypic, histological and molecular analyses. Both cells were shown to differentiate successfully into adipogenic and osteogenic cell lines. Embryonic stem cell markers Pou5F1, Zpf42, FoxD3, Sox2 and Nanog were also expressed beside 5 fold higher telomerase activity in hPT-SCs that could indicate the regenerative ability of the human parathyroid gland. The osteogenic cell markers were expressed by hPT-SCs, which transformed efficiently into osteogenic cell lines, both at the level of genes (BMP2, BMP4, BGLAP, Coll11a1, Runx2, Sparc) and of proteins (BMP2, BMP4, Osteocalcin, Osteonectin, Osteopontin). Higher alkaline phosphatase (ALP) activity indicating osteogenic differentiation was determined in hPT-SCs from secondary hyperparathyroidism patients.
Conclusion: PT-SCs might responsible for the calcified parathyroid glands and other ectopic calcifications including the vascular ones, observed in the secondary hyperparathyroidism cases, beside parathyroid hormone-dependent hypercalcemia leading diffusion of calcium phosphate precipitation in tissues.

Keywords: Hyperparathyroidism; parathyroid gland; stem cells; telomerase activity and osteogenic differentiation.

1. INTRODUCTION

Mesenchymal/stromal stem cells (MSCs) were first isolated from adult bone marrow and identified as an adherent fibroblast-like population by Friedenstein and his colleagues [1]. Since then, MSCs from many other tissues have also been identified, including cord blood [2], dental pulp [3], natal teeth [4], adipose tissue [5], placenta [6], amnion [7], peripheral blood [8], pancreatic islets [9-11] and endometrium [12]. They have been shown to differentiate into multiple lineages, such as adipocytes, chondrocytes, endothelium, hepatocytes, osteocytes, myocytes, astrocytes, insulin-producing cells and neurons [13-15]. Because of these characteristics, MSCs have been accepted as important actors as in cellular therapy and tissue/organ engineering, like other somatic stem cells.

The parathyroid glands are the primary regulators of the blood calcium level by secretion of parathyroid hormone (PTH) within a controlled physiological range [16]. PTH regulates blood calcium level by several processes, including the induction of calcium release from bone into circulation, enhancing calcium abruption from the small intestine, and suppression of calcium loss in urine [17]. Several attempts have been made to identify stem/progenitors cells within parathyroid gland as a potential source for transplantable tissue [18, 19]. One of these reports indicated that stromal stem cells isolated from human parathyroid gland (hPT-SCs) represents similar phenotypic markers identical to MSCs [18]. These parathyroid-derived stem cells were previously identified as MSCs. Although they commonly behave in a very similar manner both *in vivo* and *in vitro,* they represent some individual characteristics, specific for the tissue they were isolated from. The origin and the underlying generation mechanism of these differences and their impact on biological and clinical processes are still obscure. Comparison of their differences or similarities between the various stem cell types was one of the basic approaches to understand. Those comparisons may focus on the aspects of biological marker discovery, characterization of their capacity of proliferation and differentiation along with other characteristics. Some of these cellular characteristics could be connected with the pathogenesis of diseases.

The aim of this study was to isolate and extensively characterize hPT-SCs from secondary hyperparathyroidism cases. For this purpose, proliferation capacity, telomerase enzyme activities, phenotypic properties, differentiation characteristics and gene expression profiles were analyzed and compared with mesenchymal stem cells from hBM-MSCs.

2. MATERIALS AND METHODS

2.1 Isolation of Stem Cells and Cell Culture

Human parathyroide tissues were obtained from patients who underwent surgery for secondary hyperparathyroidism. Tissue samples were obtained in accordance with a protocol approved by the institutional review board for human studies; patients provided informed consent as dictated by this protocol. Tissues were minced and digested in collagenase type II (1% (w/v), Sigma-Aldrich, St.Louis, MO, USA) to generate single cell suspensions. The cells were cultured in α-MEM (Life Sciences/GIBCO, Paisley, UK) containing 10% (v/v) fetal bovine serum (FBS; Life Sciences/GIBCO) and 100 IU/mL penicilin-100 μg/mL streptomycin (Life Sciences/GIBCO). The cells from single parathyroid gland were seeded onto two 25 cm^2 plastic tissue culture flasks (BD Labware Europe, Le Pont De Claix, France) and incubated for 3 days at 37ºC in humidified atmosphere containing 5% CO_2. Stem cells were isolated on the basis of their ability to adhere onto the culture plate. The culture medium was refreshed once every 3 days to allow further growth, in the mean time red blood cells and other non-adherent cells were removed by the way. The adherent cells grown to 70% confluency were defined as passage zero (P_0) cells. Later passages were named accordingly. For passaging, the cells were washed with Ca^{2+}-Mg^{2+} free phosphate-buffered saline (PBS) (Life Sciences/GIBCO) and detached by incubating with trypsin-EDTA solution (0.25 % (w/v), Life Sciences/GIBCO) for 5-10 min at 37ºC. Growth medium was added to inactivate trypsin. The cells were counted in duplicate using hemocytometer (Thoma), and then cultured in 75 cm^2 flasks (BD Labware Europe) at a density of 10^6cell/flask. Growth medium was replaced every 3 days over a period of 10-14 days.

Bone marrow aspirates (2–4 ml) were obtained from the iliac crest of patients (2–7 yrs old) with suspected idiopathic thrombocytopenic purpura (ITP). Informed consent was received in accordance with the terms of the ethics committee of the University of Kocaeli. Flow cytometric analysis confirmed that the donors were healthy. The bone marrow was diluted to 1:3 with PBS and layered over a Histopaque-1077 (1.077 g/ml, Sigma-Aldrich) for gradient centrifugation. The low density mononuclear cells were collected, washed twice with PBS, counted, and plated in the tissue culture flasks at a density of $1.4x10^5$ cells/cm^2 in α-MEM medium containing 10% FBS, 100 IU/ml penicillin, and 100 μg/ml streptomycin. The cells were incubated at 37ºC in a humid atmosphere containing 5% CO_2 for 3 days. On the third day, non-adherent cells were removed and fresh medium was added to allow further growth. The cultivation of cells was performed under same culture conditions defined for hPT-SCs.

2.2 Immunophenotype Analysis by FACS

To confirm that hPT-SCs and hBM-MSCs maintain their phenotypic characteristics *in vitro*, undifferentiated SCs were subjected to flow cytometry analyses. After P_3, SCs were harvested and resuspended in culture medium at a concentration of 10^6 cells/ml. Flow cytometry was performed by FACSCalibur (BD Biosciences, San Jose, CA). Data were

analyzed with CellQuest Software (BD Biosciences), and the forward and side scatter profiles were gated out of debris and dead cells.

Immunophenotyping of hPT-SCs and hBM-MSCs was performed with antibodies against the following human antigens: CD3, CD5, CD7, CD8, CD10, CD11b, CD13, CD14, CD15, CD19, CD29, CD33, CD34, CD44, CD45, CD73, CD90, CD106, CD117, CD123, CD138, CD146, CD166 and HLA-DR, HLA-ABC and HLA-G. All of the antibodies were obtained from BD Biosciences. More than 10% staining was considered as positive.

2.3 Immunohistochemical and Immunofluorescence Analysis

To identify cellular markers, cells (P_3) were seeded on poly-L-lysine coated 8-well chamber slides (BD Biosciences), cultured for another 1-2 days and subjected to immunohistochemical (IHC) and immunofluorescence (IF) analyses. In IF staining, samples were rinsed briefly in PBS, and fixed in ice-cold methanol for 10 min. After permeabilization with 0.025% Triton X-100 (Merck, Darmstadt, Germany), the cells were incubated with 1.5% blocking serum (Santa Cruz Biotechnology, Heidelberg, Germany) in PBS for 30 min at 37ºC. After washing three times with PBS (5 min each) the cells were incubated overnight at 4ºC with the primary antibodies. After three PBS washes, cells were incubated with secondary antibodies for 25 min. After washing, the cells were mounted with mounting medium containing DAPI (Santa Cruz Biotechnology).

Immunocytochemical analyses were performed using the streptavidin-peroxidase method (UltraVision Plus Large Volume Detection System Anti-Polyvalent, HRP immunostaining Kit,Thermo Scientific, UK). Cultured cells were fixed in ice-cold methanol with 0.3% hydrogen peroxide (Carlo Erba Reactifs, Val-De-Reuil Cedex Pa Des Portes, France) for 15 min. After washing step, cells were incubated with Ultra V Block for 5 min at room temperature. Then, cells were incubated overnight at 4ºC with the primary antibodies and with biotinylated secondary antibodies for 15 min at room temperature. Incubations were followed by streptavidin peroxidase treatment for 15 min at room temperature and signals were detected with the AEC kit (Zymed Laboratories, UK). The cells were counter-stained with hematoxylin (Santa Cruz Biotechnology). The list of primary antibodies was given in Table 1.

2.4 Transfection of hPT-SCs and hBM-MSCs

The cells were transfected with pGFP-N1 vector (Clontech, Palo Alto, CA, USA; constitutive expression vector with GFP gene) by Neon Transfection System (Life Sciences/Invitrogen, Carlsbad, CA). 2 x10^5 cells were mixed with 1 μg plasmid DNA, and the system was run under following parameters; 990 V/40 ms for hBM-MSCs and 1100 V/40 ms for hPT-SCs. Then, cells were cultured in α-MEM-Earle supplied with 15% FBS for 48 h. The cells were selected for 3 passages according to their resistance toward G418 (400 μg/ml). GFP^+ cells were counted after by flow cytometry. The percentage of transfected cells was determined relative to the viable cells.

Table 1. Immunocytochemical properties of hPT-SCs and hBM-MSCs

Marker	Antibody dilution	Cell Type		Marker	Antibody dilution	Cell type	
		hPT-SCs	hBM-MSCs			hPT-SCs	hBM-MSCs
CD34[2]	1:150	∅	∅	Cytokeratin 19[2]	1:50	+	+[1]
CD44[3]	1:150	+	+	MyoD[2]	1:50	∅	∅
CD45[2]	1:150	∅	∅	Myosin IIa[2]	1:50	+	+
CD71[2]	1:150	+	∅	GFAP[3]	prediluted	+	+
CD105/ Endoglin[2]	1:100	+	+	NSE/ γ-Enolase[5]	1:500	+	+
Tenascin-C[2]	1:50	+	∅	NF-M and -H[5]	1:100	+	+
CD146[4]	1:250	+	+	Vinculin[3]	1:100	+	+
HLA-DR[2]	1:50	∅	∅	Osteocalcin[2]	1:50	+	+
S100[3]	1:300	∅	∅	Osteonectin (SPARC)[5]	1:50	+	+
c-Fos[2]	1:50	+	+	Osteopontin[2]	1:50	+	+
Collagen II[3]	prediluted	+	+	BMP-2[2]	1:50	+	+
Collagen Ia1[2]	1:50	+	+	BMP-4[2]	1:50	+	+
β-Tubulin (KMX-1)[5]	1:50	+	+	Ki67[3]	1:300	+	+
β-Tubulin[3]	prediluted	+	+	PCNA[3]	1:200	+	+
Nestin[2]	1:50	+	+	Connexin 43[2]	1:100	+	+
Vimentin[2]	1:100	+	+	STAT3[3]	1:100	+	+
Desmin[3]	prediluted	+	+[1]				
Fibronectin[2]	1:100	+	+				
FSP[4]	1:100	∅	∅				
α-Smooth Muscle Actin[3]	1:800	+	+				
Actin[2]	1:50	+	+				

+= Positive marker expression; ∅= lack of marker expression;
[1]Immunoractivity was positive in 10-20% of the cells.
[2]Supplier: Santa Cruz Biotechnology, Heidelberg, Germany
[3]Supplier: Thermo Scientific, NeoMarkers, Fremont, CA, USA
[4]Supplier: Abcam, Cambridge, UK
[5]Supplier: Millipore, Temecula, CA, USA.

2.5 Gene Expression Analysis

For reverse transcriptase polymerase chain reaction (RT-PCR), total RNA was isolated from hPT-SCs and hBM-MSCs ($3x10^6$ cells) at P_3 with High Pure RNA Isolation Kit (Roche, Mannheim, Germany) and single strand cDNA was synthesized using Transcriptor High Fidelity cDNA Synthesis Kit (Roche) according to the manufacturer's instructions. For the second strand synthesis, PCR was performed using Taq DNA Polymerase (Fermentas, Vilnius, Lithuania) with primers listed in Table 2. PCR reaction mixture consisted of 1X PCR buffer, 0.2 mM dNTP, 0.5 µM of each primer, 1.25 mM $MgCl_2$ and 1.5 U Taq DNA polymerase. Following of 5 min initial denaturation step at 94ºC, genes were amplified in 30 cycles of denaturation at 94ºC/ 30 s, annealing at appropriate temperature (Table 2)/ 30s and elongation at 72ºC. The PCR reactions terminated by a final elongation step at 72ºC for 10 min. PCR products were analyzed on 1% (w/v) agarose gel.

In real-time PCR, target gene amplifications were tracked with gene specific probes (*Universal ProbeLibrary*, UPL, *Roche* Diagnostics) according to the manufacturer's recommendations on the instrument, LightCycler 480II (Roche Diagnostics).

The relative quantification of gene expressions of Nanog, Oct4, Sox2, FoxD3 and Rex1 [20] was performed with endogenous control gene, HPRT (Hypoxanthine-guanine phosphoribosyl transferase). The expression of osteogenic markers by the stem cells were analyzed with primers designed for appropriate genes: BMP2 (cggactgcggtctcctaa / ggaagcagcaacgctagaag), BMP4 (ctgcaaccgttcagaggtc / tgctcgggatggcactac), Coll11A1 (ttttccaggattcaaaggtga / tgggccaatttgaccaac), ALPL (caaccctggggaggagac / gcattggtgttgtacgtcttg), TUFT1 (ccccgagggaagatgaac / cctggagagtcagcctgaga). Results were analyzed and PCR efficiency was calculated by Light Cycler Software V.4 (Roche). The crossing points were assessed and plotted against the serial dilution of known concentrations of the standards derived from each gene by the Fit Points method. For detection of any possible DNA contamination in samples, amplification of any endogenous control genes, i.e. GAPDH, ACTA2, GUSB and Nestin were checked in Real-Time PCR.

2.6 Cell Proliferation Assay

Cell proliferation data were obtained by using xCELLigence Real-Time Cell Analyzer (RTCA) DP system (Roche Diagnostics). Cell proliferation and serum deprivation assay were performed for the detection of proliferation rate and response against serum deprivation of hPT-SCs and hBM-MSCs. This method uses impedance technology as an indicator of cell adhesion and produces electronic readout of impedance to quantify cell adhesion, proliferation and viability in real time. The presence of cells on the E-plate electrodes leads to an increase in electrode impedance, which results in a record of cell density, i.e. the cell index. The cells (12 500, 25 000 and 50 000 cell/well in 100 µl, three replica for every cell density) were inoculated into 96 E-Plates (Roche) containing 100 µl medium/well. Proliferation was monitored in real-time cell electronic sensing and the cell index (CI) was measured every 30 min for 96 h.

Table 2. Expression of markers of different lineages by hPT-SCs and hBM-MSCs assessed by RT-PCR

Gene	Primer Sequence	GeneBank acc. no.	Product Size (bp)	Expression in hPT-SCs	Expression in hBM-MSCs
ACTA2 smooth muscle actin	**F:** ATGAGGGCTATGCCTTGCCC **R:** CCCGATGAAGGATGGCTGGA	NM_001613	307	+	+
ACTB actin beta	**F:** TGGCACCACACCTTCTACAATGAGC **R:** GCACAGCTTCTCCTTAATGTCACGC	NM_001101	395	+	+
BCL3 B-cell CLL3	**F:** TCCATATTGCTGTGGTGCAGGGTA **R:** GGAGTACATTTGCGCGTTCACGTT	NM_005178	508	+	+
BGLAP osteocalcin	**F:** AGCCCTCACACTCCTCGCC **R**: GCCTCCTGAAAGCCGATGTG	NM_199173	269	+	+
BMP2 bone morphogenetic protein 2	**F:** GTGCTTCTTAGACGGACTGC **R:** GTACTAGCGACACCCACAAC	NM_001200	1232	+	+
BMP4 bone morphogenetic protein 4	**F:** AGCCATTCCGTAGTGCCATC **R:** AAGGACTGCCTGATCTCAGC	NM_130851	1374	+	+
CCR2 chemokine CC receptor 2	**F:** TTGGTGGCTGTGTTTGCTTCTGTC **R:** ATGCAGCAGTGAGTCATCCCAAGA	NM_001123041	403	+	+
CD40	**F:** AGATTGCTACAGGGGTTTCTGATAC **R:** TTTGATAAAGACCAGCACCAAGAG	NM_001250	300	+	+
CD80	**F:** GAACATCACCATCCAAGTGTCCATA **R:** TTCAGAACAACACACTCGTATGTGC	NM_005191	336	+	+
CD86	**F:** TGCACTATGGGACTGAGTAACATTC **R:** ACAGTTCAGAATTCATCTGGTGGA	NM_175862	378	∅	∅
Comp cartilage oligomeric matrix protein	**F:** CCGACAGCAACGTGGTCTT **R:** CAGGTTGGCCCAGATGATG	NM_000095	91	+	+
CX3CR1 chemokine CX3-C receptor 1	**F:** TCACCGTCATCAGCATTGATAGGTA **R:** AACAGCGTCTGGATGATTCTGAAGT	NM_001337	298	+	+
DES desmin	**F:** CAGGTGGAGATGGACATGTCTAAGC **R:** TCATCTCCTGCTTGGCCTGG	NM_001927	186	+	+
c-FOS FBJ murine osteosarcoma viral oncogene	**F:** AGAATCCGAAGGGAAAGGAA **R:** CTTCTCCTTCAGCAGGTTGG	NM_005252	149	+	+
HLA-DRB4 MHC complex, class II, DRB4	**F:** TTGGAGCAGGCTAAGTGTGAGTG **R:** TCCGAGGAACTGTTTCCAGCATC	NM_021983	477	∅	∅

Gene	Primer Sequence	GeneBank acc. no.	Product Size (bp)	Expression in hPT-SCs	Expression in hBM-MSCs
IFNG interferon, gamma	**F:** GCATCCAAAAGAGTGTGGAG **R:** GCAGGCAGGACAACCATTAC	NM_00619	254	**-/+**	∅
IL10 interleukin 10	**F:** TGAGAACCAAGACCCAGACA **R:** TCATGGCTTTGTAGATGCCT	NM_000572	181	**-/+**	∅
IL12A interleukin 12A	**F:** AGCCTCCTCCTTGTCGCTACC **R:** GCCTCCACTGTGCTGGTTTTATC	NM_000882	235	**-/+**	+
IL6R interleukin 6 receptor	**F:** GAGGGAGACAGCTCTTTCTAC **R:** CCGTTCAGCCCGATATCTGAG	NM_000565	239	+	+
MAPKAPK2 Map kinase-activated protein kinase2	**F:** TCATGAAGAGCATCGGTGAG **R:** TCAAAGAGTTGTGGCTGGTG	NM_032960	165	+	+
MGLL monoglyceride lipase	**F:** CAATCCTGAATCTGCAACAACTTTC **R:** ATGTTTATTTCATGGAAGACGGAGT	NM_007283	411	+	+
MYOG myogenin	**F:** TATGAGACATCCCCCTACTTCTACC **R:** CTTCTTGAGCCTGCGCTTCT	NM_002479	279	+	+
NANOG	**F:** CCTCTTAAATTTTTTCCTCCTCTTC **R:** AAGTGGGTTGTTTGCCTTTG	NM_24864	271	-/+	+
NCF1 neutrophil cytosolic factor1	**F:** CCTTCATCCGTCACATCGCC **R:** TGATCGCCCCTGCCTCAATA	NM_000265	185	+	+
NES nestin	**F:** CTCTGACCTGTCAGAAGAAT **R:** GACGCTGACACTTACAGAAT	NM_006617	302	+	+
OCT4 /POU5F1	**F:** TGCCGTGAAACTGAAGAAG **R:** TTTCTGCAGAGCTTTGATGTTC	NM_203289	72	+	+
PLIN2 adipophilin	**F:** CGCTGTCACTGGGGCAAAAGA **R:** ATCCGACTCCCCAAGACTGTGTTA	NM_001122	173	+	+
PPARG peroxisome proliferator-activated receptor gamma	**F:** CAGTGGGGATGCTCATAA **R:** CTTTTGGCATACTCTGTGAT	NM_138711	422	+	+
REX-1 /ZFP42	**F:** GGATCTCCCACCTTTCCAAG **R:** GCAGGTAGCACACCTCCTG	NM_020695	104	+	+
RUNX2 runt-related transcription factor 2	**F:** CAGACCAGCAGCACTCCATA **R:** CAGCGTCAACACCATCATTC	NM_004348	177	+	+
SOX2	**F:** ATGGGTTCGGTGGTCAAGT	NM_003106	133	+	+

Gene	Primer Sequence	GeneBank acc. no.	Product Size (bp)	Expression in hPT-SCs	Expression in hBM-MSCs
SRY-box 2	**R:** GGCGCCGTGGGAGATACATG				
SOX9 SRY-box 9	**F:** TGAAGAAGGAGAGCGAGGAA **R:** GGGGCTGGTACTTGTAATCG	NM_000346	348	+	+
SPARC osteonectin	**F:** TCTTCCCTGTACACTGGCAGTTC **R:** AGCTCGGTGTGGGAGAGGTA	NM_003118	73	+	+
TGFB1 transforming growth factor beta 1	**F:** GTGGAAACCCACAACGAAATCTA **R:** ATCGCCAGGAATTGTTGCTGTAT	NM_000660	201	+	+
TNFAIP3 tumor necrosis factor, alpha-induced protein3	**F:** GTATTTGAGCAATATGCGGAAAGC **R:** TCCTGAGATTTGAGAGACTCCAGTT	NM_006290	420	+	+
VIM vimentin	**F:** AAGCAGGAGTCCACTGAGTACC **R:** GAAGGTGACGAGCCATTTCC	NM_003380	205	+	+

+= *Positive marker expression; -/+= Weak expression; ∅= lack of marker expression*

2.7 Telomerase Activity

Telomerase activity was determined by conventional telomeric repeat amplification protocol (TRAP) using TeloTAGGG PCR-ELISA kit (Roche) according to the manufacturer's protocol. Briefly, after lysis of 2×10^5 cells, 3 μl of supernatant was incubated with pre-mixed buffer to show the presumed telomerase activity for 20 min at 25ºC and the products were amplified with biotin-labeled primers by PCR. Streptavidin coated ELISA plates were used to quantify the activity by addition of peroxidase specific substrate (3,3',5,5'-Tetramethylbenzidine dihydrochloride; TMB) and reading the optical density at 450 nm. Relative telomerase activity (RTA) was calculated with respect to the control template equivalent to 0.001 mol/μl DNA.

2.8 *In vitro* Differentiation

To induce adipogenic differentiation, cells were seeded onto 6-well plates (3000 cells/cm^2) and cultured with Mesencult MSC Basal Medium supplemented with 10% adipogenic supplement (StemCell Technologies Inc., Vancouver, BC, Canada) and 1% penicillin/streptomycin for 3 weeks. The medium was refreshed every 2-4 days. Intracellular lipid droplets indicating adipogenic differentiation confirmed by Oil Red O staining with 0.5 % oil red O (Sigma-Aldrich) in methanol.

For osteogenic differentiation, cells (P_3; 3000 cells/cm^2) were seeded onto collagen (type I) precoated coverslips in 6-well plates. The differentiation medium (MEM-Earle supplemented with 0.1 μM dexamethasone (Sigma-Aldrich), 0.05 μM ascorbate-2-phosphate (Wako Chemicals, Richmond, VA, USA), 10 mM β-glycerophosphate (Sigma-Aldrich), 1% antibiotic/antimycotic and 10% FBS) was replaced twice a week. After four weeks, osteogenic differentiation was assessed by alkaline phosphatase activity and alizarin red staining. For Alizarin Red staining, cells were fixed for 5 min in ice-cold 70% ethanol. The cells were stained with alizarin red solution (2%, pH 4.2) for 30s. Stained cells were dehydrated in pure acetone, fixed in acetone-xylene (1:1) solution, cleared with xylene.

Alkaline phosphatase (ALP) activity was determined to confirm the osteogenic differentiation. Cell layers were washed three times with PBS and total protein was extracted by Mammalian Protein Extract Reagent (M-PER; Thermo Scientic). Cells were incubated at room temperature with p-Nitrophenyl Phosphate Substrate (Sigma Aldrich) for 30 min. The optical density was determined at 405 nm. Protein concentration of the cell lysate was measured by bicinchoninic acid assay (BSA, Sigma-Aldrich). The lysate was incubated at 60ºC for 30 min with BCA working solution and the color change was measured at 562 nm. Three technical replicates of each sample were analyzed.

To induce neurogenic differentiation, cells (P_3) seeded on type I collagen coated cover slips were cultivated until 70% confluence was attained. Then, cells were cultured for 3-5 days in differentiation medium (MEM-Earle supplemented with 0.5 mM isobutylmethylxanthine (IBMX), 10 ng/ml brain-derived neurotrophic factor (BDNF), epidermal growth factor (EGF), basic fibroblast growth factor (β-FGF), neural stem cell proliferation supplements (Stem Cell Technologies) and 1% penicillin-streptomycin). Differentiation was assessed by IHC staining of GFAP, HNK-1ST, neurofilament (Thermo Scientific), tubulin-β, tubulin-βIII, c-Fos, nestin and γ-enolase (Santa Cruz Biotechnology).

2.9 Statistical Analysis

All experiments were repeated minimum of three times. Data were reported as means ±SD. All statistical analyses were performed using SPSS 10.0 (SPSS Inc., Chicago, IL, USA). Data were analyzed using one-way ANOVA and un-paired *t*-test. Differences between the experimental and control groups were regarded as statistically significant when *P=0.05* and lower.

3. RESULTS

3.1 Cell Culture of hPT-SCs and hBM-MSCs

In the first days of the culture of isolated cells, two distinct cell types were observed attached on the plastic surface of the flask: endocrine cells of parathyroidea gland with epithelial morphology, and fibroblast like cells (Fig. 1A). But, in the following passages, the ratio of these cells were increased (Fig. 1B), and expanded such that the surface of the culture flask was covered by these cells (Fig. 1C, 1D). The endocrine-like cells with epithelial morphology were eliminated in further passages. No changes in morphology or growth pattern were observed throughout 10 passages. Moreover, cells demonstrated high vitality and capability to restart proliferation, and are capable of retaining their differentiation potential after a long-term storage at -80ºC.

Like hPT-SCs, hBM-MSCs also displayed a fibroblast-like, spindle-shaped morphology during the early days of incubation. These primary cells reached to 70-80% confluency after 12-15 days of incubation in early passages. In following passages, most of the cell morphology became large, flattened or fibroblast-like (data not shown).

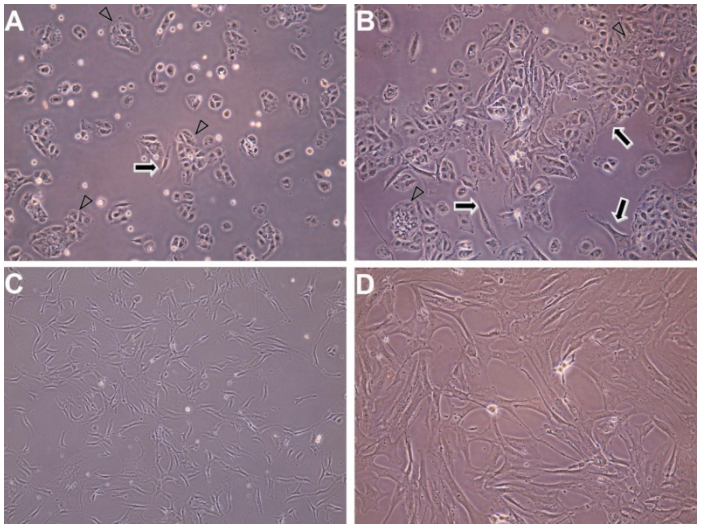

Fig. 1. Development of hPT-SC line

During the onset of the culture in the P0 and 2nd day (A), Progress of the cell cultures in P0-5th day (B) and in P1-7th day (C). The cell lineage were fully developed on P4-4th day, on which the cells exhibited large, flattened or fibroblast-like morphology (D). The solid arrows indicate the presence of stromal mesenchymal stem cells and the arrowheads (triangular) show the location of epithelial cells of parathyroidea gland (Orginal magnification, X100 for B, C and X200 for A, D).

3.2 Characterization of Hpt-Scs by Flow Cytometry

Pre-defined markers that specify MSCs together with others were used to define the immunophenotypic characteristics of cultured cells. The results indicated that hPT-SCs expressed all MSC markers; but not CD3, CD5, CD7, CD8, CD10, CD11b, CD14, CD15, CD33, CD34, CD45, CD106, CD117, CD123, CD138, HLA-G or HLA-DR (Fig. 2A, 2B). The marker expression profile of hPT-SCs and hBM-MSCs were very similar, but the expression of CD44 was much lower in hPT-SCs (Fig. 2B).

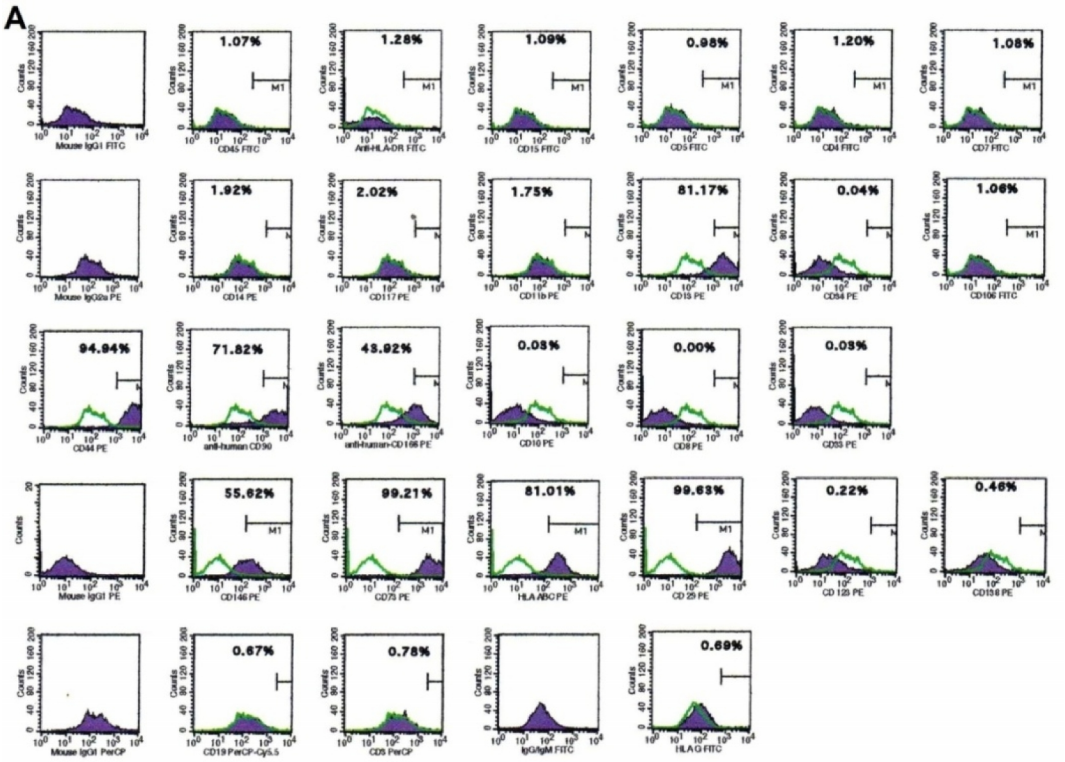

B

Marker	Expression (%)		Marker	Expression (%)	
	hPT-SCs	hBM-MSCs		hPT-SCs	hBM-MSCs
CD3	0.88±0.53	1.09±1.06	CD45	0.78±0.35	1.77±0.11
CD5	0.64±0.51	1.58±0.66	CD73	99.37±0.22	99.05±1.11
CD7	0.60±0.53	1.79±0.74	CD90	74.71±4.09	97.91±1.51
CD8	0.02±0.03	0.64±0.77	CD106	0.84±0.71	6.48±1.94
CD10	0.08±0.05	1.22±0.86	CD117	1.93±0.11	1.02±0.60
CD11b	1.90±0.30	1.31±0.86	CD123	0.10±0.11	0.76±1.03
CD13	76.91±4.11	96.82±1.37	CD138	0.17±0.25	0.50±0.55
CD14	1.66±0.28	1.17±1.00	CD146	51.70±5.55	32.81±0.22
CD15	0.67±0.40	1.71±0.61	CD166	74.79±2.40	98.03±1.21
CD29	99.58±0.07	98.98±0.68	HLA-ABC	79.09±2.72	69.12±2.73
CD33	0.11±0.13	0.83±1.03	HLA-DR	0.95±0.30	2.54±1.08
CD34	3.59±3.40	0.70±0.90	HLA-G	3.39±3.36	6.03±1.69
CD19	0.90±0.76	1.17±1.23			
CD44	37.22±3.22	98.09±1.18			

Fig. 2. Representative flow cytometry analysis of cell-surface markers in hPT-SCs at P3 (A). The purple area shows the reading of respective markers, and the green line indicates the isotype control. Immunophenotypic properties of hPT-SCs and hBM-MSCs by flow cytometry (B)

3.3 Immunocytochemical Characterization of hPT-SCs

The immunocytochemical staining results of hPT-SCs are shown in Fig. 3 and Fig. 4, and comparative immunoreactivity profile for both cell lines was given in Table 1. Under standard culture conditions, these cells expressed MSC markers, such as CD105 (Fig. 4G), fibronectin (Fig. 3A) and CD44 (data not shown), without altering their morphological characteristics. Vimentin, one of the most used cytoplasmic markers to describe MSCs, was expressed throughout the passages in both cells (Fig. 4E). None of the cell lines were stained with surface markers CD34 (Fig. 3D), CD45, HLA-DR, CD117 (data not shown) and FSP (Fig. 3B).

We observed expression of osteoblastic markers, like type-I, osteocalcin, osteopontin, BMP-2 (data not shown), BMP-4 (Fig. 4K) and osteonectin (Fig. 4J) in undifferentiated hPT-SCs. In addition, hPT-SCs expressed some of the myogenic markers, including α-smooth muscle actin (ACTA2; Fig. 4A), myosinIIa (data not shown) and desmin (Fig. 4B). Conversely, hPT-SCs did not stained by antibody against MyoD (data not shown).

Remarkably, GFAP (an intermediate filament protein specific for astroglial cells) (Fig. 3G) and other neural stem/progenitor markers, i.e. nestin (data not shown), vimentin (Fig. 4E), tenascin (Fig. 4C), and neuronal markers, i.e. c-fos (data not shown), Eno2 (Fig. 4I) and neurofilament (NF)-H (Fig. 3I) were expressed by hPT-SCs.

hPT-SCs also showed positive staining for Ki-67, STAT3 (signal transducer and activator of transcription 3) (data not shown), connexin-43 (Fig. 4D), vinculin (Fig. 4F), CD146 (Fig. 4H) and PCNA (proliferating cell nuclear antigen) (Fig. 4L). hPT-SCs were positive for CK-19 (Fig. 3E) while were showing negative expression for CK18 (Fig. 3F). The expression patterns of most of the mentioned markers in both cell lines were common. However, only a subpopulation in the hBM-MSCs culture was stained positive for CK-19 (Table 1). In addition, hBM-MSCs did not stain with antibody against tenascin and CD71 (Table 1). GFP^+ hPT-SCs could be visualized under fluorescence microscope without immunostaining after transfection with GFP gene (Fig. 3H).

3.4 Gene Expression Profiles of hPT-SCs

The expressions of the stemness and differentiation markers were confirmed in hPT-SCs by RT-PCR analysis using specific primer sets (Fig.5, Table 2). The expressions of Rex-1, Oct4, Sox2 and Nanog were identified in both hPT-SCs and hBM-MSCs. As the multipotency and the proliferation are under the control of these key transcription factors in mammals, their expressions might indicate stemness characteristics of cells. In addition, the expression of differentiation markers of precursor osteoblasts, such as osteonectin (Sparc), osteocalcin (Bglap), osteopontin and Runx2; adipoblast markers adipophilin (Plin2) and Pparg; Acta2 and desmin (Des); myogenin (Myog), part of gene family regulating myogenesis; precursor neuroprogenitor cell marker nestin (Nes) were detected. The presence of cartilage oligomeric matrix protein (Comp) and Sox9 which is expressed in precursor chondroblasts expressions were also observed in hPT-SCs. The results demonstrated that hPT-SCs show characteristical mesenchymal stem cell properties.

HLA-DRB4 and CD86 expressions were not observed in both cell lines. Interestingly, IL2, IL10 and interferon gamma (IFNg) were weakly expressed by hPT-SCs while they are not

expressed in hBM-MSCs at all. In addition, co-stimulatory molecules, CD80 and CD40 were expressed in both hPT-SCs and hBM-MSCs.

The expression of the embryonic stem cell genes, i.e. Rex-1, Oct4, Nanog, Sox2 and FoxD3 was confirmed by real-time PCR (Fig. 6). Data showed that Nanog, Oct4, FoxD3 and Sox2 were expressed at higher levels in hBM-MSCs, while only Rex1expression was slightly higher in hPT-SCs. To check any DNA contamination in samples, primers for GAPDH, ACTA2, GUSB and Nestin were used for amplification of any possible DNA residue in RNA isolation samples, but no amplification was observed.

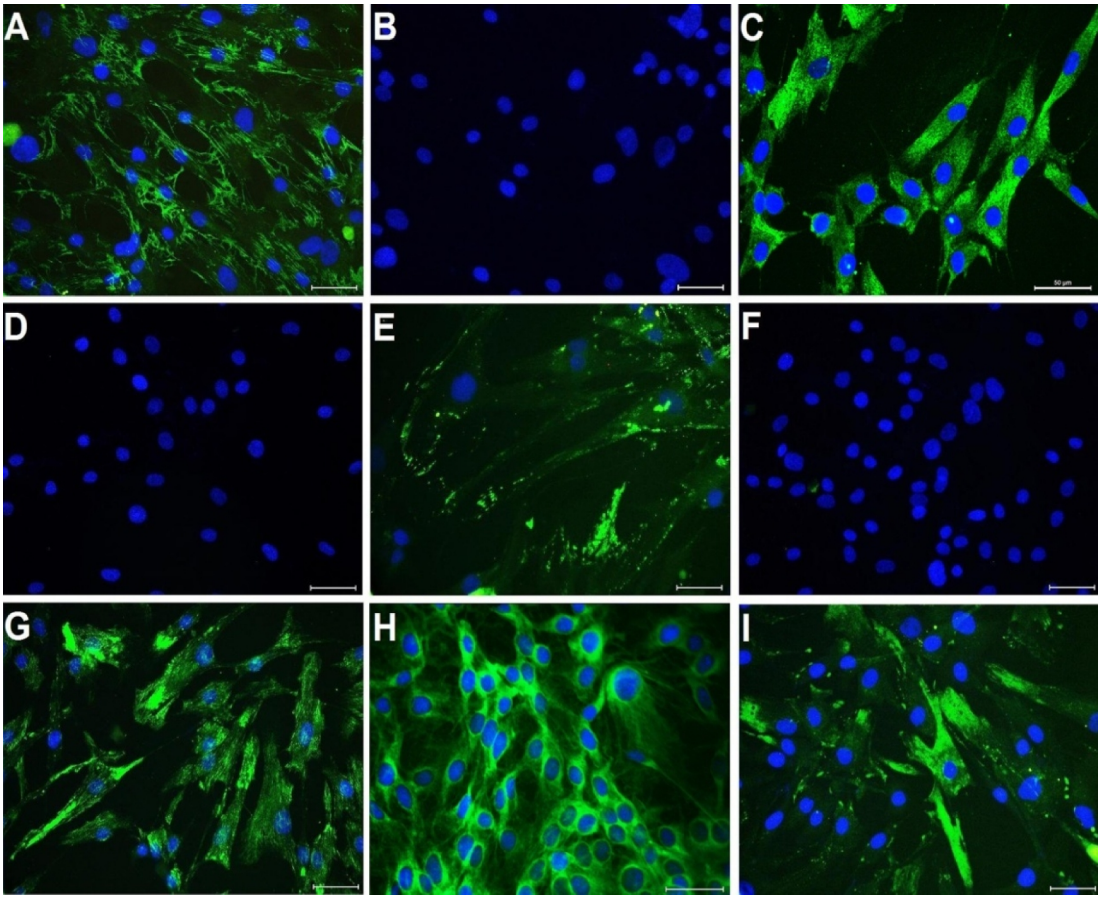

Fig. 3. **Immunofluorescence analysis for expression of some markers**

Expression of fibronectin (A), CD71 (C), CK19 (E), GFAP (G) and NF (I) were detected. hPT-SCs did not stain positive with antibody against FSP (B), CD34 (D), and CK18 (F) . GFP^+ cells after transfection of hPT-SCs without immunostaining (H). Nuclei were labeled with DAPI (blue) (Scale bars= 30 μm).

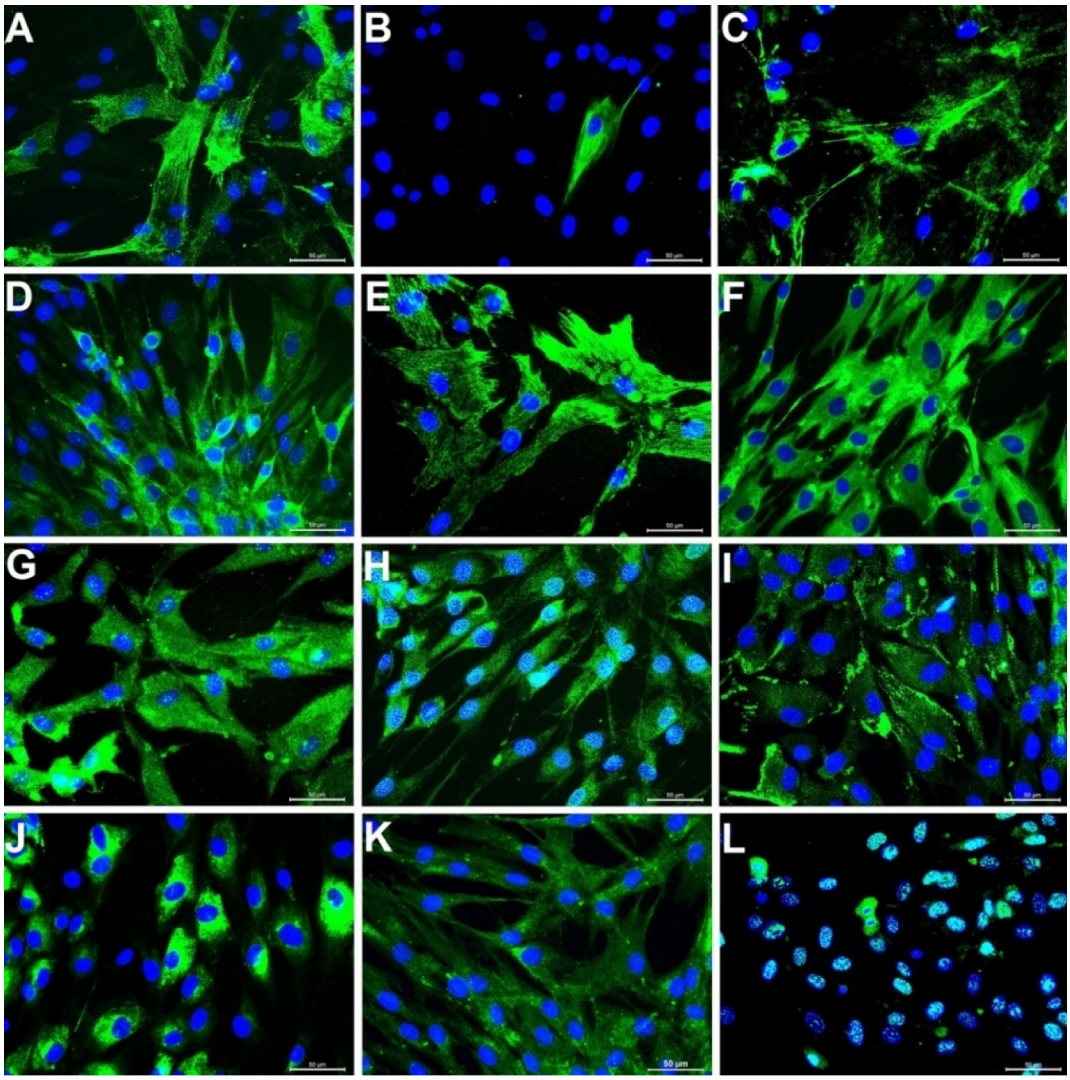

Fig. 4. ***The immunofluorescence appearances of the cells incubated with ASMA2 (A), Desmin (B), Tenascin (C) Connexin-43 (D), Vimentin (E), Vinculin (F), Endoglin (CD105) (G), CD146 (H), Eno2 (I), Osteonectin (J), BMP-4 (K) and PCNA (L) primary antibodies. Interestingly, ASMA2 present most cells while desmin expressed by some cells. Tenascin, Connexin-43, Vinculin and Eno2 showed either cytoplasmic membrane or cytoplasmic pattern which showed heterogeneous expression with positive within hPT-SCs cultures. Osteonectin showed granular intracellular expression, while PCNA labeled in a nuclear pattern in hPT-SCs. Nuclei are labeled with DAPI (blue). Scale bars= 50μm***

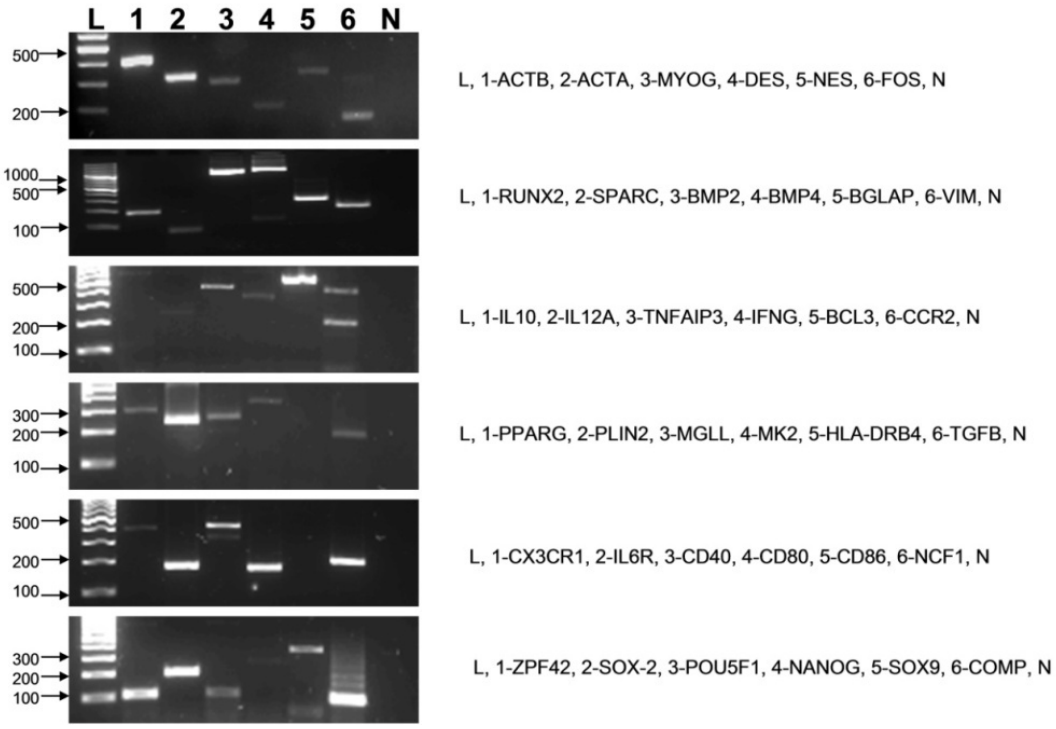

Fig. 5. Agarose gel electrophoresis of RT-PCR products

Representative panel of RT-PCR analysis of hPT-SCs for expression profile of embryonic stem cell genes and differentiation markers. Embryonic stem cell (Rex-1,Oct4, Nanog, Sox2) and differentiation (ASMA2, Desmin, NEF-H, NEF-L, b3-tubulin, Eno2, Nestin, Osteopontin (SPP1), Osteocalcin (BGLAP), Runx-2, Osteonectin (SPARC), Adipophilin (PLIN2)and PPARg)markers was verified. The expressions were normalized with respect to the expression of ß-actin. Reactions without cDNA were used for negative control.

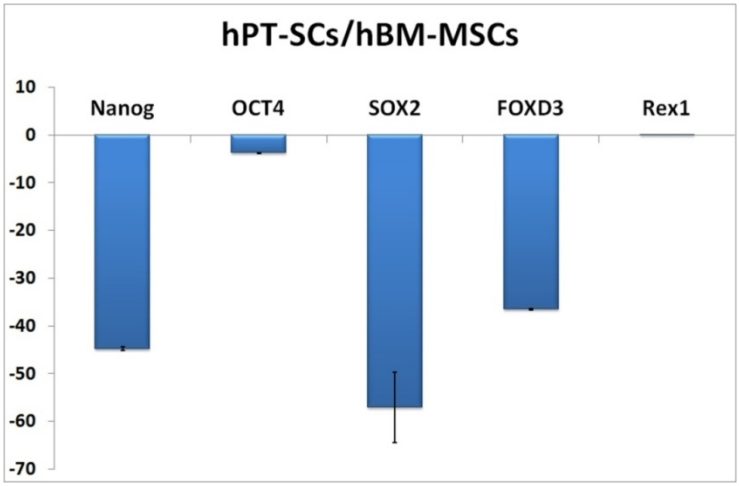

Fig. 6. Quantitative gene expression analysis of hPT-SCs by Real Time PCR in comparison with the hBM-MSCs

3.5 Differentiation Potential of hPT-SCs

hPT-SCs differentiated into adipogenic, osteogenic and neurogenic lineages under proper conditions and the transformations were proven by histochemical and IHC methods. For adipogenic differentiation, 80-90% sub-confluent hPT-SCs culture (P_3) was induced (Fig.7A,B). After about 3 weeks, lipid droplets appeared and invaded the entire cytoplasm like in adipocytes (Fig. 7A). Lipid droplets stained with Oil Red O (Fig. 7B). Lipid droplet formation was not observed in control group (Supplementary Fig. 1).

To assess the osteogenic differentiation of hPT-SCs and hBM-MSCs cultivated in differentiation medium, markers specific for bones were analyzed (Fig.7C,D). After 10 days, the cellular aggregates were observed in osteogenic differentiation culture and gradually increased. These nodular aggregates were characterized by deposits of amorphous material, which stained by alizarin red S that signify the presence of calcium deposits (Fig. 7C). Alizarin red positive nodular aggregates were observable after about 20 days, and osteocalcin, osteonectin, osteopontin, BMP2 and BMP4 immunoreactions (Fig. 8) were much intense than undifferentiated cells. On the other hand, control cultures showed only minimal background staining of Alizarin red (Supplementary Fig. 2). ALP activity, another osteogenic differentiation indicator, increased in both cell lines in osteogenic differentiation medium following 7 days of incubation. The activity level stayed constant until 14^{th} day and decreased later. Remarkably, the ALP level in hPT-SCs was higher than hBM-MSCs (Fig. 9A). The expression of gene markers for osteogenic differentiation (BMP2, BMP4, Coll11A1, BGLAP, Runx2 and Sparc) was quantified for both cell lines by Real-Time PCR (Fig. 9B). hBM-MSCs expressed all these markers moderately. Whereas, hPT-SCs showed very strong expression of BMP2 and BGLAP.

Neuron-like cells derived from hPT-SCs within 48 h of induction, displaying distinctive morphologies that range from extensively simple bipolar to large, branched multipolar cells (Fig.10). To confirm their neuronal characteristics, differentiated cells were stained for neuron/glial cell specific markers: TUBB3, GFAP, c-FOS, NF, HNK1ST (Fig.10 C, D, E1-E4, F1-F4), ENO2, MAP2a,b and NES (data not shown). Besides their morphological changes into neuron/glial like cells, the immunostaining showed the intensifying of all neuronal markers during differentiation. This observation might be the result of the cytoplasmic shrinkage. However, noticeable increase in both nuclear and cytoplasmic expressions, especially in c-FOS, was indicative of high cellular activity towards differentiation (Fig. 10 F3, F4).

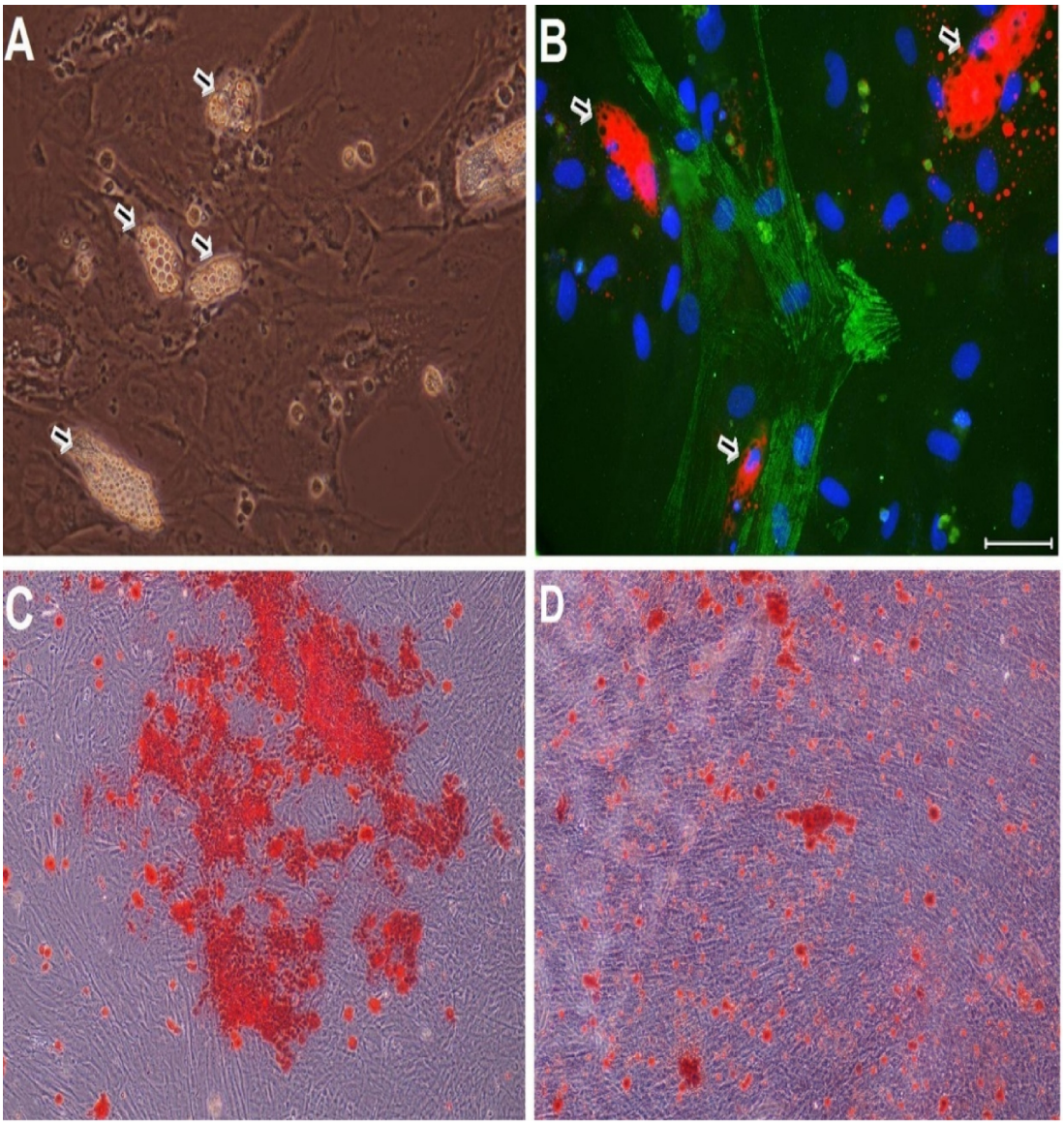

Fig. 7. Differentiation potential of hPT-SCs into adipogenic and osteogenic lineages

Adipocytes were induced from hPT-SCs (A-B). Presence of the lipid clusters were detected by phase-contrast microscopy at the day 20 (arrows) (A). Intracellular lipid accumulation, which was used to mark adipocyte differentiation, was determined by Oil red O staining (arrows) on 16th day, and ASMA2 expression was shown in green and nuclei in blue with DAPI (B). . Osteogenic differentiation was indicated by the formation of calcified nodule with Alizarin red S staining in hPT-SCs (C) and hBM-MSCs (D). The calcified nodule appeared bright red in color (Original magnification: A,B=X400; C,D=X40).

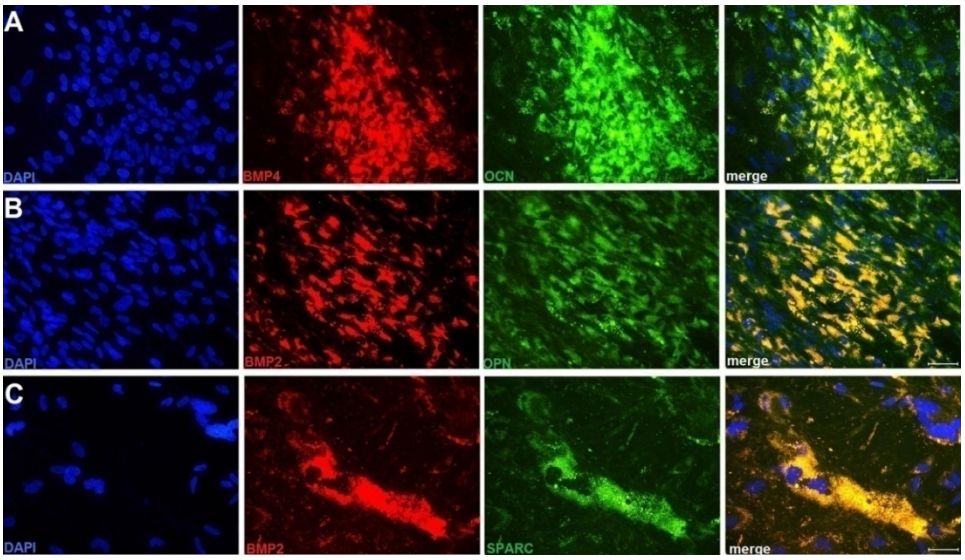

Fig. 8. Immunofluoresence analysis of osteogenic differentiation

After differentiation progress, the samples were stained against the osteogenic protein markers BMP2, BMP4, Osteocalcin, Osteopontin and SPARC.

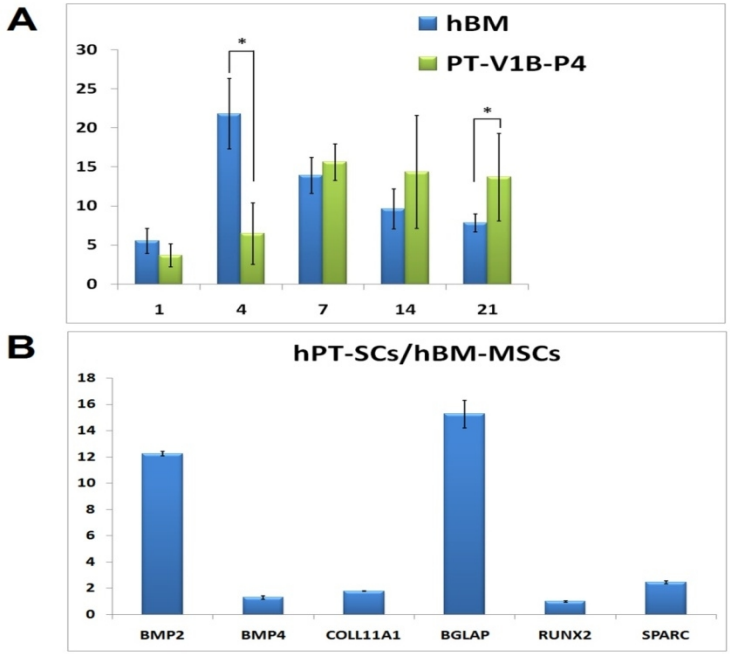

Fig. 9. Osteogenic differentiation of hPT-SCs and hBM-MSCs

(A) The alkaline phosphatase activity during the osteogenic differentiation of both cell lines. The activities were represented in terms of the mol p-nitrophenol/min/mg protein (, P=0.05). (B) The expression of gene markers for osteogenic differentiation (BMP2, BMP4,Coll11A1, BGLAP, RUNX2 and SPARC) was quantified for both cell lines by Real-Time PCR.*

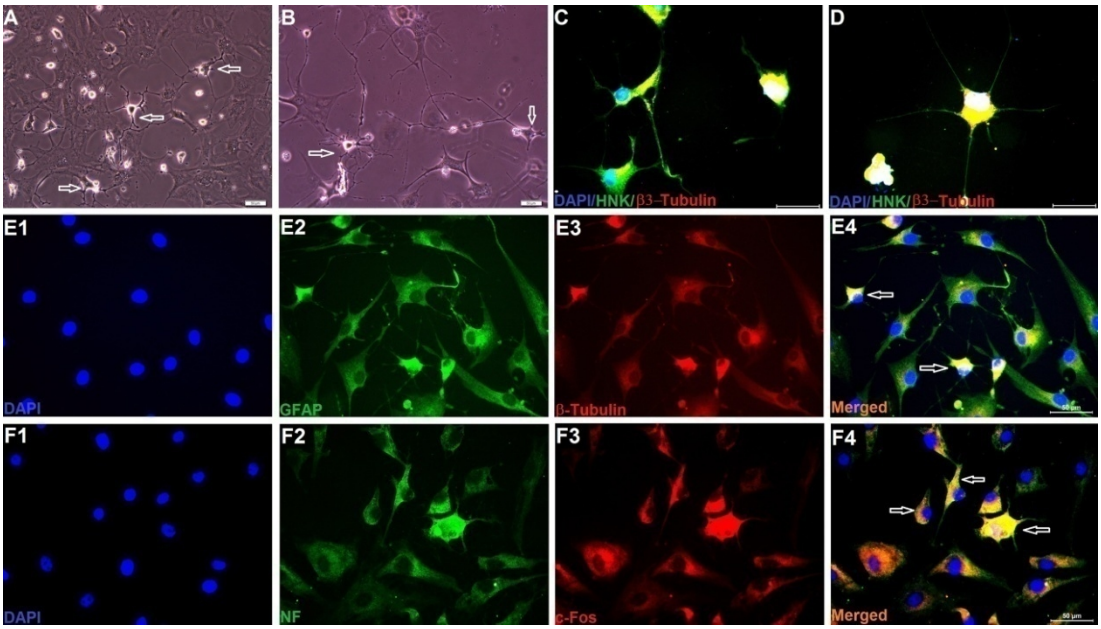

Fig. 10. Differentiation of hPT-SCs to neuronal lineage

Under phase contrast microscope, hPT-SCs-derived neuron-like cells displayed distinct morphologies, ranging from extensively simple bipolar to large, branched multipolar cells (arrows) (A,B). Differentiated cells robustly expressed both HNK and Tubb3 which are specific for neuronal cells (C,D). GFAP (E2) and Tubb (E3) were strongly positive throughout the perikarya and extensions (arrows). NF was detected as discontinuities along the cells (arrows) and c-Fos can be detected as nuclear and perinuclear pattern in cells (arrows) (F1-F4). Scale bars = 50 µm.

3.6 Growth Characteristic and Telomerase Activity of hPT-SCs

The adult stem cells isolated from parathyroid and bone marrow of human possessed considerable amount of telomerase activity (Fig. 11). In addition, cells isolated from parathyroid gland had almost 5 times as much telomerase activity as the cells isolated from bone marrow indicating the regenerative ability of the human parathyroid gland. Cell proliferation data were obtained by using xCELLigence Real-Time Cell Analyzer (RTCA) DP system (Roche Diagnostics). Cell proliferation and serum deprivation assay were performed for the detection of proliferation rate and response against serum deprivation of hPT-SCs and hBM-MSCs. The proliferation data represented a higher growth rate of hPT-SCs than hBM-MSCs in the media supplemented with serum (Fig. 12 A1, B1). The cells, however, show different cell index profile in the serum-free media (Fig. 12 A2, B2). Serum deprivation is a potent inducer of apoptosis in cell culture. Specific cytokines, like EGF, protect certain cell types from the induction of apoptosis due to the elevated production of intracellular reactive oxygen intermediates (ROIs) coupled with decreased levels of intracellular and extracellular antioxidants. To show the resistance differences of cells against the ROIs, serum deprivation assay was used.

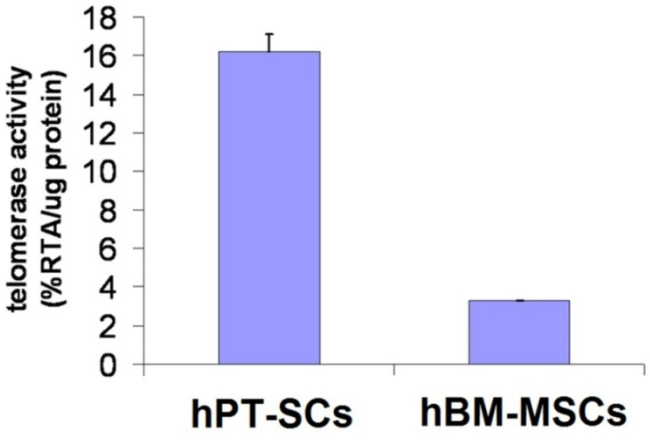

Fig. 11. Telomerase activities of hPT-SCs and hBM-MSCs

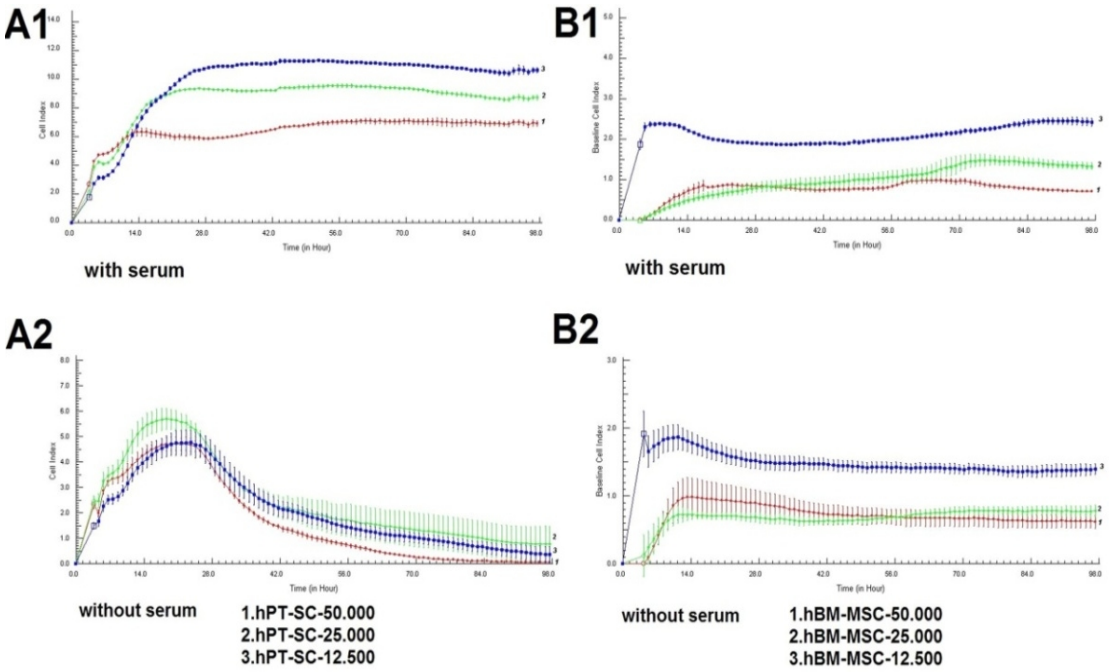

Fig. 12. ***Dynamic proliferation curves for hPT-SCs and hBM-MSCs seeded at 12 500, 25 000 and 50 000 cells per well (A1, B1). To show the serum deprivation, the same set was repeated for the media without serum supplementation (A2, B2). Cell growth is assessed with the xCELLigence system that measures electrical impedance across micro-electrodes integrated on the bottom of tissue culture E-96 plates. Impedance measurements are displayed as Cell Index (CI) values, providing real-time quantitative information on cell growth. As it was shown in A1 and B1 that hPT-SCs had more proliferation capacity than hBM-MSCs. Whereas hBM-MSCs were more resistant under serum free conditions***

4. DISCUSSION

For the first time, Shih et al. reported stem cells isolated from the PT *in vitro* [18]. In this report, plastic-adherent, fibroblast-like cells from parathyroid glands were isolated and grown in culture. The surface phenotype of these cells were found to be positive for CD73, CD166, CD29, CD49a, CD49b, CD49d, CD44, CD105, and MHC class I, and negative for CD34, CD133, CD117, CD114, CD31, CD62P, EGF-R, ICAM-3, CD26, CXCR4, CD106, CD90 and MHC class II, similar to MSCs. In the present study, PT-SCs derived from PT attached to culture flasks sparsely, and the majority of the cells displayed a fibroblast-like, spindle-shaped morphology during the early days of incubation. These cells began to proliferate in approximately 3-4 days and gradually grew to form small colonies, as designated “colony forming units”. Besides, they express CD13, CD29, CD44, CD73, CD90, CD146, CD166 and HLA-ABC, but not CD3, CD5, CD7, CD8, CD10, CD11b, CD14, CD15, CD19, CD33, CD34, CD45, CD106, CD117, CD123, CD138 or HLA-DR, we also showed that PT-SCs could differentiate into adipocytes, osteoblasts, and neuron-like cells. For that reason, they could be classified as MSCs based on the criteria above.

Telomerase activity is usually in correlation with proliferation characteristic and maturity. Since adult stem cells play critical roles in tissue regeneration and maintenance, the limitation of their life span by replicative senescence due to the lack of the enzyme activity affects the biological structures and functions, also called “aging”. Although cells from different tissues could show quite different activities, the age still remains an important determinant. Despite of the absence of telomerase activity in most of the somatic cells, stem cells and germ cell lines conserved their telomerase activity to some degree with their proliferation capacity. In prior study by Shih et al., detectable levels of telomerase activity were observed from the isolated PT-SCs [18]. Similarly, telomerase activity was found to be positive both for PT-SCs and hBM-MSCs used in this study. However, the activity was remarkably higher in PT-SCs, approximately 6 times, despite these cells were compared with the hBM-MSCs derived from the younger individual. The high telomerase activity of PT-SCs was correlated significantly with the cell proliferation data. In our previous study, the telomerase activity could not be detected even in hBM-MSCs from older individuals [20], and it has been determined that this activity was closely related with the age of the individuals, which the tissue was derived from. In this study, PT-SCs were obtained from Secondary hyperparathyroidism (SHPT) samples, which are characterized by pronounced parathyroid gland hyperplasia. The increase of the size of the gland could not be associated only with the increase of the number of the gland cells, but the stromal stem cells could also play an important role, as well. The high proliferation rate and increased telomerase activity could provide sufficient evidence that those cells might have affected by the conditions causing the SHPT. Indeed, the telomerase activity and proliferation of those cells should be compared with those of PT-SCs from healthy individuals, to justify their role played in disease progress. Although telomerase activity was previously checked in healthy, hyperplastic and malignant parathyroid tissues, and it was determined that it was only detectable in malignant tumors [21-23], our results showed that this activity should also be checked in stem cells of healthy parathyroid tissue. However, those samples could not be obtained easily due to the ethical regulations. Alternatively, those assays could be repeated with the samples obtained from cadavers.

STAT3 was activated by stress, growth factors and cytokines in a wide range of tissues and organs as an important factor in cellular processes, like TNFR2-mediated cell survival, apoptosis, proliferation, inflammation and angiogenesis [24-27]. This indicated that STAT3 expression in hPT-SCs maintains their proliferative and undifferentiated state.

Moreover, the expression of MAPKAPK2, TNIP1 and BCL3 genes in hPT-SCs could be connected with their role in the anti-apoptotic effects. MAPKAPK2 (Mitogen-activated protein kinase-activated protein kinase 2) is a direct substrate of p38 MAP kinase in response to cellular stress [28], and TNIP1 (tumor necrosis factor induced protein 3 interacting protein 1) was known as an anti-apoptotic TNF-α-induced gene in endothelial cells [29]. Besides, BCL3 can activate the cell cycle regulator cyclin D1 and the anti-apoptotic BCL2 proteins [30]. Expression of these three genes might implicate their role in the anti-apoptotic influence mechanisms and their protective role in the localized tissues or organs.

The modulation of immune response at multiple levels by MSCs was demonstrated on regeneration and function of both $CD34^+$ and monocyte-derived dentritic cells [31]. However, IFNg stimulated MSCs could act as antigen presenting cells and activated immune responses [32-34]. The expression of antigen presenting surface proteins CD40, CD80, CD86 and MHC class-II were analyzed, and it was found that CD40 and CD80 were expressed by hPT-SCs and hBM-MSCs without stimulation. However, CD86 expression could not be detected in both cell lines, as in other studies [35,36]. Moreover, hPT-SCs and hBM-MSCs also did not express MHC Class II, whose expression was confined to professional antigen presenting cells (APCs) of the immune system. This might indicate both cells might involve in the activation of antigen-specific immune responses facultative APCs.

SHPT refers to the excessive secretion of PTH by the parathyroid glands in response to hypocalcemia (low blood calcium levels) and associated hypertrophy of the glands. SHPT is one of the most important complications in chronic kidney disease (CKD) [37]. High PTH levels are responsible for the increased number and activity of osteoclasts, and also for the increased bone resorption in CKD. The clinical manifestation of SHPT includes bone deformities, broken bones (fractures) and swollen joints. In addition, hyperplasia and calcification of all four parathyroid glands in a young female hemodialysis patient with severe secondary hyperparathyroidism have been reported with supporting computerized tomography and histological findings [38]. Moreover, metastatic calcification in primary hyperparathyroidism after parathyroid carcinoma (PT-Ca) has been reported by Kawashima et al. in multiple tissues, including lung, myocardial fibers and renal tubules in two cases, despite this phenomenon is well-known in long-term complication of chronic renal failure accompanied with secondary hyperparathyroidism [39]. Recently, it has been revealed that parathyroid hormone-related protein contributed in the vascular calcification of chronic hemodialysis patients [40].

The mechanisms underlying the accelerated vascular calcification in CKD are not completely understood. Changes in the arterial wall, fibro-elastic intimae thickening, calcification of elastic lamellae, increased extracellular matrix, deposition of collagen and relatively small elastic fiber content are all well known to cause arterial remodeling in CKD patients. Many bone-associated proteins, including osteocalcin, osteopontin and osteoprotegerin, and many bone morphogenetic proteins, are involved in the remodeling process, and they are expressed in calcified arterial lesions and are associated with vascular calcification [41, 42].

It was previously proposed that all perivascular cells are actually MSCs and distributed throughout the body as pericytes [43]. Perivascular cells also do not express CD31 or CD45 explaining why MSCs can be isolated from all tissues which are present throughout the entire organism. In fact, the presence of stem-like cells in the wall of vasculature was noticed for the first time 40 years ago [43]. For instance, pericytes, which were originally defined by their morphology and close contact to endothelial cells, can differentiate into other cell types, including osteoblasts, chondrocytes, adipocytes, fibroblasts, myofibroblasts and smooth

muscle cells, which are properties shared also by MSCs [44-49]. Presently, no “pan-specific” marker is available to define pericyte phenotype unambiguously. Commonly used markers such as CD146, NG2, Desmin, Asma2 and the regulator of G-protein signaling RGS5 label the heterogeneous pericyte population [44, 45, 50]. In the current study, hPT-SCs expressed markers that were also accepted as specific markers for pericytes including CD146, Desmin, Asma2, CD29, CD44, CD90, CD105, Vimentin and Collagen type-1. Both cells, i.e. mesenchymal stem cells and pericytes, have some common characteristics. We are in the opinion that pericytes might actually be the MSCs that were located in perivascular area, and this was supported by other studies [44,47,50,51].

Noticeably, the markers for ostegenic differentiation were expressed by two cell lines both at the level of genes (BMP2, BMP4, Osteocalcin, Coll11a1, Runx2 and Osteonectin) and of proteins (BMP2, BMP4, Osteocalcin, Osteonectin and Osteopontin). It was found that both cell lines were successfully induced for the osteogenic differentiation. In addition to these, high level of gene expression related with the osteogenic differentiation in hPT-SCs from secondary hyperparathyroidism patients was estimated by the Real-Time PCR. Higher alkaline phosphatase (ALP) activities in hPT-SC supported this idea. From this point of fact, it could be considered that these perivascular area stem cells with MSC character in parathyroid gland might responsible for the calcified parathyroid glands and other ectopic calcifications including the vascular ones, observed in the secondary hyperparathyroidism cases, beside parathyroid hormone-dependent hypercalcemia leading diffusion of calcium phosphate precipitation in tissues.

ACKNOWLEDGEMENTS

We thank Alparslan Okcu and Cansu Subası for their excellent technical assistance. The authors have declared that no conflict of interest exists.

CONSENT

All authors declare that written informed consent was obtained from the patient for publication of this report.

ETHICAL APPROVAL

All authors hereby declare that all experiments have been examined and approved by the appropriate ethics committee and have therefore been performed in accordance with the ethical standards laid down in the 1964 Declaration of Helsinki.

COMPETING INTERESTS

Authors have declared that no competing interests exist.

REFERENCES

1. Luria EA, Panasyuk AF, Friedenstein AY. Fibroblast colony formation from monolayer cultures of blood-cells. Transfusion. 1971;11(6):345-49.
2. Erices A, Conget P, Minguell JJ. Mesenchymal progenitor cells in human umbilical cord blood. British Journal of Haematology. 2000;109(1):235-42.

3. Pierdomenico L, Bonsi L, Calvitti M, Rondelli D, Arpinati M, Chirumbolo G, et al. Multipotent mesenchymal stem cells with immunosuppressive activity can be easily isolated from dental pulp. Transplantation. 2005;80(6):836-42.
4. Karaoz E, Dogan BN, Aksoy A, Gacar G, Akyuz S, Ayhan S, et al. Isolation and *in vitro* characterisation of dental pulp stem cells from natal teeth. Histochemistry and Cell Biology. 2010;133(1):95-112.
5. Zuk PA, Zhu M, Mizuno H, Huang J, Futrell JW, Katz AJ, et al. Multilineage cells from human adipose tissue: Implications for cell-based therapies. Tissue Engineering. 2001;7(2):211-28.
6. Anker PSI, Noort WA, Scherjon SA, Kleuburg-van der Keur C, Kruisselbrink AB, van Bezoolien RL, et al. Mesenchymal stem cells in human second-trimester bone marrow, liver, lung, and spleen exhibit a similar immunophenotype but a heterogeneous multilineage differentiation potential. Haematologica. 2003;88(8):845-852.
7. in 'tAnker PS, Scherjon SA, Kleijburg-van der Keur C, Noort WA, Claas FHJ, Willemze R, et al. Amniotic fluid as a novel source of mesenchymal stem cells for therapeutic transplantation. Blood. 2003;102(4):1548-9.
8. Villaron EM, Almeida J, Lopez-Holgado N, Alcoceba M, Sanchez-Abarca LI, Sanchez-Guijo FM, et al. Mesenchymal stem cells are present in peripheral blood and can engraft after allogeneic hematopoietic stem cell transplantation. Haematologica. 2004;89(12):1421-7.
9. Karaoz E, Ayhan S, Gacar G, Aksoy A, Duruksu G, Okcu A, et al. Isolation and characterization of stem cells from pancreatic islet: pluripotency, differentiation potential and ultrastructural characteristics. Cytotherapy. 2010;12(3):288-U19.
10. Karaoz E, Genc ZS, Demircan PC, Aksoy A, Duruksu G. Protection of rat pancreatic islet function and viability by coculture with rat bone marrow-derived mesenchymal stem cells. Cell Death and Disease. 2010;1.
11. Karaoz E, Okcu A, Saglam O, Genc ZS, Ayhan S, Kasap M. Pancreatic islet derived stem cells can express co-stimulatory molecules of antigen-presenting cells. Transplantation proceedings. 2010;42(9):3663-70.
12. Musina RA, Belyavski AV, Tarusova OV, Solovyova EV, Sukhikh GT. Endometrial Mesenchymal Stem Cells Isolated from the Menstrual Blood. Bulletin of Experimental Biology and Medicine. 2008;145(4):539-43.
13. Pittenger MF, Mackay AM, Beck SC, Jaiswal RK, Douglas R, Mosca JD, et al. Multilineage potential of adult human mesenchymal stem cells. Science. 1999;284(5411):143-7.
14. Prockop DJ. Marrow stromal cells as stem cells for continual renewal of nonhematopoietic tissues and as potential vectors for gene therapy. Journal of Cellular Biochemistry. 1998;284-5.
15. Lee OK, Kuo TK, Chen WM, Lee KD, Hsieh SL, Chen TH. Isolation of multipotent mesenchymal stem cells from umbilical cord blood. Blood. 2004;103(5):1669-75.
16. Brown EM. Extracellular Ca2+ Sensing, Regulation of Parathyroid Cell-Function, and Role of Ca2+ and Other Ions as Extracellular (1st) Messengers. Physiological Reviews. 1991;71(2):371-411.
17. Potts JT. Parathyroid hormone: past and present. Journal of Endocrinology. 2005;187(3):311-25.
18. Shih YRV, Kuo TK, Yang AH, Lee OK, Lee CH. Isolation and characterization of stem cells from the human parathyroid gland. Cell Proliferation. 2009;42(4):461-70.
19. Fang SH, Guidroz JA, O'Malley Y, Lal G, Sugg SL, Howe JR, et al. Expansion of a cell population expressing stem cell markers in parathyroid glands from patients with hyperparathyroidism. Annals of Surgery. 2010;251(1):107-13.

20. Duruksu G, Aksoy A, Okcu A, Karaoz E. Comparative analysis of telomerase activities of mesenchymal stem cells isolated from different human tissues. Haematologica. 2010;95(Suppl.2):661.
21. Onoda N, Ogisawa K, Ishikawa T, Takenaka C, Tahara H, Inaba M, et al. Telomerase activation and expression of its catalytic subunits in benign and malignant tumors of the parathyroid. Surgery Today. 2004;34(5):389-93.
22. Kammori M, Nakamura KI, Ogawa T, Mafune KI, Tatutomi Y, Obara T, et al. Demonstration of human telomerase reverse transcriptase (hTERT) in human parathyroid tumours by in situ hybridization with a new oligonucleotide probe. Clinical Endocrinology. 2003;58(1):43-8.
23. Velin AK, Herder A, Johansson KJM, Trulsson LM, Smeds S. Telomerase is not activated in human hyperplastic and adenomatous parathyroid tissue. European Journal of Endocrinology. 2001;145(2):161-164.
24. Fu XY. STAT3 in immune responses and inflammatory bowel diseases. Cell Research. 2006;16(2):214-9.
25. Niu GL, Wright KL, Huang M, Song LX, Haura E, Turkson J, et al. Constitutive Stat3 activity up-regulates VEGF expression and tumor angiogenesis. Oncogene. 2002;21(13):2000-8.
26. Wei DY, Le XD, Zheng LZ, Wang LW, Frey JA, Gao AC, et al. Stat3 activation regulates the expression of vascular endothelial growth factor and human pancreatic cancer angiogenesis and metastasis. Oncogene. 2003;22(3):319-29.
27. Wang MJ, Zhang WJ, Crisostomo P, Markel T, Meldrum KK, Fu XY, et al. STAT3 mediates bone marrow mesenchymal stem cell VEGF production. Journal of Molecular and Cellular Cardiology. 2007;42(6):1009-15.
28. Ono K, Han JH. The p38 signal transduction pathway - Activation and function. Cellular Signalling. 2000;12(1):1-13.
29. Opipari AW, Boguski MS, Dixit VM. The A20 Cdna Induced by Tumor Necrosis Factor-Alpha Encodes a Novel Type of Zinc Finger Protein. Journal of Biological Chemistry. 1990;265(25):14705-8.
30. Kashatus D, Cogswell P, Baldwin AS. Expression of the Bcl-3 proto-oncogene suppresses p53 activation. Genes and Development. 2006;20(2):225-35.
31. Nauta AJ, Kruisselbrink AB, Lurvink E, Willemze R, Fibbe WE. Mesenchymal stem cells inhibit generation and function of both CD34(+)-derived and monocyte-derived dendritic cells. Journal of Immunology. 2006;177(4):2080-7.
32. Stagg J, Pommey S, Eliopoulos N, Galipeau J. Interferon-gamma-stimulated marrow stromal cells: a new type of nonhematopoietic antigen-presenting cell. Blood. 2006;107(6):2570-7.
33. Chan JL, Tang KC, Patel AP, Bonilla LM, Pierobon N, Ponzio NM, et al. Antigen-presenting property of mesenchymal stem cells occurs during a narrow window at low levels of interferon-gamma. Blood. 2006;107(12):4817-24.
34. Morandi F, Raffaghello L, Bianchi G, Meloni F, Salis A, Millo E, et al. Immunogenicity of human mesenchymal stem cells in HLA-class I-restricted T-Cell responses against viral or tumor-associated antigens. Stem Cells. 2008;26(5):1275-87.
35. Tse WT, Pendleton JD, Beyer WM, Egalka MC, Guinan EC. Suppression of allogeneic T-cell proliferation by human marrow stromal cells: Implications in transplantation. Transplantation. 2003;75(3):389-97.
36. Zhao DC, Lei JX, Chen R, Yu WH, Zhang XM, Li SN, et al. Bone marrow-derived mesenchymal stem cells protect against experimental liver fibrosis in rats. World Journal of Gastroenterology. 2005;11(22):3431-40.

37. Sumida K, Nakamura M, Ubara Y, Marui Y, Tanaka K, Takaichi K, et al. Histopathological alterations of the parathyroid glands in haemodialysis patients with secondary hyperparathyroidism refractory to cinacalcet hydrochloride. Journal of Clinical Pathology. 2011;64(9):756-60.
38. Peces R, Rodriguez M, Gonzalez F, Ablanedo P. Calcification of all four parathyroid glands in a hemodialysis patient with secondary hyperparathyroidism revealed by computerized tomography. Scandinavian Journal of Urology and Nephrology. 2001;35(4):328-9.
39. Kawashima J, Watanabe E, Sada K, Yamada S, Shimoda S, Tsuruzoe K, et al. Two cases with metastatic calcification in parathyroid carcinoma. Endocr Rev. 2011;32(3):237.
40. Liu F, Fu P, Fan W, Gou R, Huang Y, Qiu H, et al. Involvement of Parathyroid Hormone-Related Protein in Vascular Calcification of Chronic Hemodialysis Patients. Nephrology (Carlton). 2012. doi: 10.1111/j.1440-1797.2012.01601.x.
41. Nitta K. Vascular Calcification in Patients with chronic kidney disease. Therapeutic Apheresis and Dialysis. 2011;15(6):513-21.
42. Jono S, Shioi A, Ikari Y, Nishizawa Y. Vascular calcification in chronic kidney disease. Journal of Bone and Mineral Metabolism. 2006;24(2):176-81.
43. Abedin M, Tintut Y, Demer LL. Mesenchymal stem cells and the artery wall. Circulation Research. 2004;95(7):671-676.
44. Meirelles LDS, Chagastelles PC, Nardi NB. Mesenchymal stem cells reside in virtually all post-natal organs and tissues. Journal of Cell Science. 2006;119(11):2204-13.
45. Bergers G, Song S. The role of pericytes in blood-vessel formation and maintenance. Neuro-Oncology. 2005;7(4):452-464.
46. Brachvogel B, Moch H, Pausch F, Schlotzer-Schrehardt U, Hofmann C, Hallmann R, et al. Perivascular cells expressing annexin A5 define a novel mesenchymal stem cell-like population with the capacity to differentiate into multiple mesenchymal lineages. Development. 2005;132(11):2657-68.
47. Zannettino ACW, Paton S, Arthur A, Khor F, Itescu S, Gimble JM, et al. Multipotential human adipose-derived stromal stem cells exhibit a perivascular phenotype *in vitro* and *in vivo*. Journal of Cellular Physiology. 2008;214(2):413-21.
48. Crisan M, Yap S, Casteilla L, Chen CW, Corselli M, Park TS, et al. A perivascular origin for mesenchymal stem cells in multiple human organs. Cell Stem Cell. 2008;3(3):301-13.
49. Tintut Y, Alfonso Z, Saini T, Radcliff K, Watson K, Bostrom K, et al. Multilineage potential of cells from the artery wall. Circulation. 2003;108(20):2505-10.
50. Meirelles LD, Caplan AI, Nardi NB. In search of the in vivo identity of mesenchymal stem cells. Stem Cells. 2008;26(9):2287-99.
51. Hoshino A, Chiba H, Nagai K, Ishii G, Ochiai A. Human vascular adventitial fibroblasts contain mesenchymal stem/progenitor cells. Biochemical and Biophysical Research Communications. 2008;368(2):305-10.

Peer-review history:
The peer review history for this paper can be accessed here:
http://www.sciencedomain.org/review-history.php?iid=194&id=12&aid=996